Preparation, morphology and sonication time dependence of silver nanoparticles in amphiphilic block copolymers of PEO with polystyrene or PMMA

Imad-Ud-Din[b], Mohsan Nawaz[a], Gareth J. Price[c], Musa Kaleem Baloch[b], Masroor Ahmad Bangesh[a], Wajid Rehman[a], Hameed Ullah[a] and Saeed Ahmad[b]

[a]*Department of Chemistry, Hazara University, Mansehra, Pakistan*

[b]*Institute of Chemical Sciences, Gomal University, Dera Ismail Khan, Pakistan*

[c]*Department of Chemistry, University of Bath, Claverton Down, Bath, BA2 7AY, UK*

[d]*Department of Chemistry, University of Malakand, Chakdara, Pakistan*

Abstract

Composite materials comprising arrays of silver nanoparticles in amphiphilic copolymers have been prepared by sonochemically enhanced borohydride reduction of precursor silver nitrate ($AgNO_3$). The precursor was incorporated into the cores of polymeric micelles formed from block copolymers of polystyrene (PS) or poly(methyl methacrylate) (PMMA) with poly(ethylene oxide) (PEO). The copolymers were synthesised with varying hydrophobic block lengths from a PEO macroinitiator by atom transfer radical polymerization (ATRP). UV/visible spectroscopy was used to confirm the formation of elemental silver and the effect of sonication time on the appearance of the silver nanoparticles was determined. The growth was faster than when gold nanoparticles are formed in comparable block copolymers. Nanoparticles formed in copolymers with PMMA blocks were more stable to agglomeration than when polystyrene was used. Electron microscopy revealed the morphology of the nanocomposites which confirmed that both block copolymers are vehicles for the formation of well-defined films containing nanoparticulate silver. However, AgNP formation shows some significant differences from previous reports of gold NP containing materials formed under similar conditions.

Keywords: Nanoparticles, block copolymer, ultrasound, silver, sonication time.

Introduction

Nanotechnology can be defined as the design, production and application of materials and devices with at least one dimension in the nanometer scale [1]. Nanoparticles (NPs) offer unique properties not found in bulk materials. Many examples have been reported concerning metallic NPs being used as catalysts [2] as well as exploiting their size-dependent optical and electronic properties [3, 4]. Silver nanoparticles (AgNPs) are emerging as one of the fastest growing product categories in the nanotechnology industry with great potential in the fields of medicine and biology for their potent antibacterial and antifungal activities [5, 6]. They are also being used in clothing, paints, coatings, cosmetics, and electronics, as well as in the food industry [7]. Their extremely small size allows easy interaction with other particles and matrices, leading to increased antibacterial efficiency such that 1 g of AgNPs can confer antibacterial properties to several hundred square meters of substrate material.

AgNPs can be synthesized using various methods including chemical, photochemical or electrochemical reaction or γ-radiation of suitable substrates or laser ablation [8]. The most widely used is the reduction of silver salts by sodium borohydride or sodium citrate. This preparation is simple, but great care must be exercised to make stable and reproducible colloids [9, 10]. Other reducing agents have been used, including natural, more benign reagents such as gelatin or starch [11]. The use of ultrasound to enhance the reactions has also been shown to be beneficial [12, 13] and to allow some control over the size and shape of the NPs. However, there remains a need for simple and more direct methods to control the synthesis in order to readily generate the required morphology and properties as well as to control adsorption onto appropriate substrates. For example, fabrication of electronic devices often requires structured arrays containing nanometer sized metal or semiconductor particles separated by non-conductive

barriers [14] in a periodic structure. Most physical nanofabrication techniques such as electron-beam or scanning probe lithography are costly and time consuming if used to produce large-scale devices. A wide range of techniques have been used to incorporate the nanoparticles into different solid media such as glass, ceramics, textiles and polymers [15] although NPs prepared using small molecule surfactants or which have adsorbed ions can undergo agglomeration or be difficult to disperse in a hydrophobic matrix. Using amphiphilic block copolymers (BCPs) gives a potentially attractive method to overcome some of these deficiencies.

BCPs form a variety of nanometre-sized, micro phase-separated structures by self-organisation, depending on the relative block lengths and the relative interactions between each block [16]. In an appropriate solvent, an amphiphilic BCP forms micelles with a soluble shell and insoluble hydrophilic core into which metal salts or inorganic particles can partition and react to form nanoparticles.

Block copolymer micelles with cores containing ethylene oxide or vinyl pyridine have been used to stabilize gold and silver nanoparticles grown from an aqueous solution. They form films in which the particles are homogeneously dispersed [17, 18]. More recently, syntheses of materials with more complex architectures such as amphiphilic double-cylinder-type brushes and their composites with AgNPs [19] using poly(methacrylic acid–*co*-methyl methacrylate) have been reported. Star copolymers with multi arm blocks can form single molecules with hydrophilic cores in which NPs can be formed [2]. Since the AgNPs are stabilized *e.g*. with a hydrophobic PMMA corona, such nanocomposites are compatible with organic solvents and polymers.

The self-organization of block copolymers is sensitive to their environment, including the solvent or the inorganic precursor. Particle and film formation is often accompanied by complex

transformations of the equilibrium structure of the copolymer. In order to avoid this loss in structural control, we chose an approach where the kinetic stability of the micelles formed in dilute solution was sufficient to be retained after removal of the solvent from cast films [20].

In a previous paper, we reported the synthesis of gold nanoparticles (AuNPs) using ultrasound and their incorporation in amphiphilic PS-*b*-PEO block copolymer matrices [21]. That work showed a crucial dependence of nanoparticle yield and size on the reaction time. The aim of the work described here was to prepare nanostructured composite films containing AgNPs. Atom transfer radical polymerization (ATRP) was used to synthesize further amphiphilic diblock copolymers of poly(ethylene oxide), with either polystyrene, PS-*b*-PEO, or poly(methyl methacrylate), PMMA-*b*-PEO, with varying block lengths. AgNPs were generated in the hydrophilic PEO cores of the polymer micelles in solution by partition of a silver salt [17] followed by chemical reduction. However, while applying the sonochemical reduction method employed by Möller and co-workers, [20, 22] a strong dependence of the resulting silver nanoparticle size on sonication conditions was noted so that this work also investigates these issues with an aim of controlling and optimizing the reaction conditions and highlighting differences from the methods used for gold containing systems.

Experimental

Materials

All the chemicals and reagents used were purchased from Aldrich. Poly(ethylene oxide) monomethyl ether (MePEO) 5000 was dried by azeotropic distillation with toluene on a water separator. α-chlorophenylacetylchloride was distilled over a Vigreux column. Inhibitors in styrene (St) and methyl methacrylate (MMA) were removed by passage through the appropriate

inhibitor removal columns. Copper (I) bromide (98%), 2,2-bipyridine (bipy), silver nitrate (≥ 99.0%) and sodium borohydride were all used as received. Polymerization was carried out in an inert gas atmosphere using nitrogen (Linde) gas which was passed over molecular sieves (4Å) and finely distributed potassium on aluminium oxide.

Preparation and characterization of block copolymers

Preparation of the PEO macroinitiator and its copolymerization with styrene, summarized in Scheme 1, has previously been described in detail [21, 23]. Three PEO–*b*-PS block copolymers (**1** – **3**) with fixed PEO block length and varying amounts of styrene were prepared. Three PEO–*b*-PMMA (**4** – **6**) copolymers were prepared using a similar process as summarized in Scheme 1. The appropriate amounts of MMA (ca. 35 mmol), initiator, CuBr and bipy were filled into a Schlenk tube and degassed by three freeze-thaw cycles before filling with nitrogen and immersing in an oil bath at 130 ^{o}C. Polymerization was terminated by cooling rapidly to room temperature. The product was dissolved in 40 cm^3 dichloromethane and precipitated into a mixture of 30 cm^3 of 0.5% HCl and 450 cm^3 of cold methanol. The polymer was isolated by filtration and dried to constant weight. Varying the ratio of macroinitiator to MMA gave block copolymers with different hydrophobic block lengths. The macroinitiator and block copolymers were characterized by ^{1}H NMR, using Bruker Avance 250 and 300 MHz spectrometers with $CDCl_3$ as solvent. The block copolymer composition was determined by the ratio of the NMR signal intensity of the phenyl peak region (St) or that of the ester methyls (MMA) to that of the alkyl PEO region. The number (M_n), and weight (M_w) average molecular weights were estimated by GPC using THF at room temperature with a flow rate of 1 cm^3 min^{-1}. Calibration was based on polystyrene or PMMA standards as appropriate.

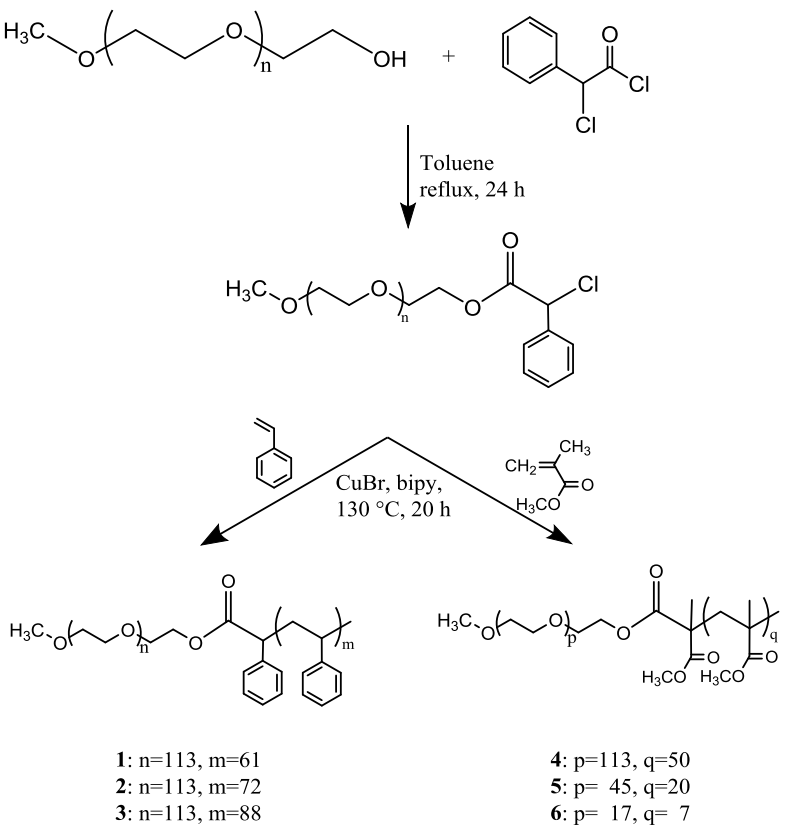

1: n=113, m=61
2: n=113, m=72
3: n=113, m=88

4: p=113, q=50
5: p= 45, q=20
6: p= 17, q= 7

Scheme 1

Synthesis of Silver Nanoparticles

Solutions of 1% (w/w) PS-*b*-PEO or PMMA-*b*-PEO were prepared in toluene. $AgNO_3$ (0.1 - 0.3 equivalents of $AgNO_3$ per EO) was added and sonicated using a cleaning bath (30 kHz, delivering 0.4 W of power into the reaction) for 1 h to obtain a transparent solution. Solid sodium borohydride ($NaBH_4$, ca. 0.05 g) was then added and sonication continued for a further 1 h during which the solution turned yellow-orange before ending up a deep purple colour. The formation of elemental silver was confirmed by UV/Vis absorption spectroscopy using an Agilent 8453 UV-Visible Spectrophotometer with a 1.0 cm path length quartz cuvette, monitoring the presence of a peak around 410 nm.

Transmission Electron Microscopy (TEM)

One drop of a diluted solution of block copolymer in toluene was placed on a carbon-coated copper grid and the solvent allowed to evaporate. TEM micrographs (JEOL JEM 1200, 80 kV) were recorded. In order to minimize charging and damage to the polymer, the electron beam intensity was kept as low as feasible.

Scanning Electronic Microscopy (SEM)

Several drops of the final micelle/NP solution (concentration ~ 0.1%) in toluene were placed in an aluminium pan and the solvent allowed to evaporate in a dust-free environment. Scanning electronic micrographs (JEOL JSM.6480LV) were recorded at a variety of magnifications after coating with gold.

Results and Discussion

Atom transfer radical polymerization (ATRP) has previously been used to produce a variety of functional polymers and copolymers [24]. Building on previous use to produce PS-*b*-PEO materials, the macroinitiator formed by reacting hydroxyl-terminated PEO polymer with an ATRP active end group was also used to polymerise methyl methacrylate. The properties of each of the materials are shown in Table 1. The syntheses proceeded as expected except for **6** which produced, on average, a shorter MMA block but broader polydispersity than suggested by the ratio of the reactants. The GPC indicated that this sample had an element of bimodality in the distribution, containing a small proportion of a polymer with a lower molecular weight of ~1700. The yields of copolymer were somewhat higher for PMMA-*b*-PEO than for PS-*b*-PEO.The

physical and thermal properties of the copolymers and their phase behaviour have been reported and discussed elsewhere [25].

Table 1. GPC molecular weights (M_n) and polydispersity index (*PDI*) of the copolymers

Sample	Composition	M_n / g mol^{-1}	PDI
1	PS_{61}-*b*-PEO_{113}	11300	1.29
2	PS_{72}-*b*-PEO_{113}	12500	1.21
3	PS_{88}-*b*-PEO_{113}	14200	1.18
4	$PMMA_{50}$-*b*-PEO_{113}	14400	1.08
5	$PMMA_{20}$-*b*-PEO_{45}	13800	1.10
6	$PMMA_{7}$-*b*-PEO_{17}	4570	2.78

Solutions of each of the block copolymers were prepared in toluene at concentrations well above the critical micelle concentration [21]. Silver nitrate ($AgNO_3$) was added which partitioned into the micelle interior under gentle sonication for 1h. At this point, the solution remained transparent with no absorbance in the visible region indicating that no silver nanoparticles had formed.

Following addition of $NaBH_4$, continued sonication at low intensity resulted in the colour of the solution changing from colourless to deep-purple/black over the course of 1 h. The formation of AgNPs was confirmed by the absorption spectra, shown for PS_{61}-*b*-PEO_{113} in Figure 1(a). The typical plasmon resonance for silver was observed at around 420 nm [26]. This absorption wavelength suggests that the mean particle size is in the range of 20 – 30 nm and the spectra indicate that this stays consistent throughout the sonication. Generally, a lower maximum absorption wavelength indicates a smaller average size of the AgNPs. The spectra for the silver

nanoparticles in the three (PS-*b*-PEO) block copolymer samples were similar to Figure 1(a) with each having an absorption maximum around 410 - 420 nm. Also of interest is the time dependence of the spectra. Figure 1(a) indicates that for Ag in PS-*b*-PEO, the absorbance increased only very slightly after the first 20 min of reaction. Further reaction time was of little or no benefit, despite there being examples in the Literature of extended durations being used. Significantly, the wavelength of maximum absorption did not change, indicating that the average particle size remained essentially unchanged.

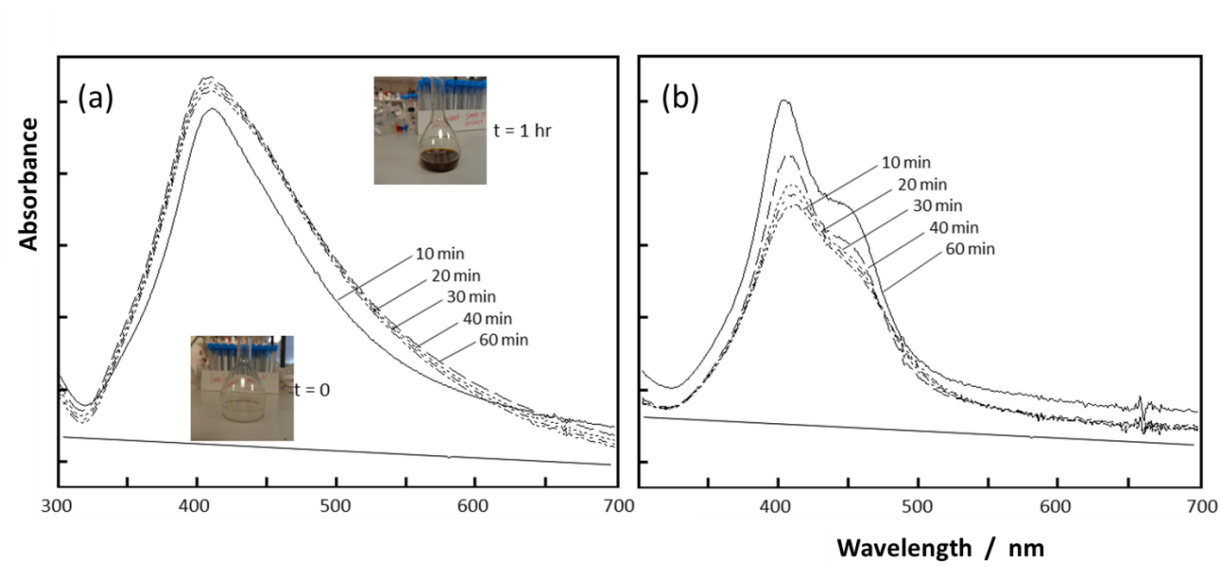

Fig. 1. Absorbance spectra for reduction of $AgNO_3$ at the indicated sonication times after addition of $NaBH_4$. (a) PS_{61}-*b*-PEO_{113} (the insets show the colours of the solutions before sonication and after 1 h). (b) $PMMA_7$-b-PEO_{17}. The spectrum at t = 0 was recorded immediately prior to adding the $NaBH_4$.

Somewhat different behavior was noted when the hydrophilic block was changed to PMMA. For $PMMA_{50}$-*b*-PEO_{113} *i.e.* the same size block of PEO and a long block of PMMA, the appearance of the spectrum was again similar to Figure 1(a).The main difference was that the growth of the absorption peak continued throughout the 1 h sonication rather than stopping after a certain time. It has previously been reported that silver nanoparticles grow more slowly than

gold under comparable conditions [27] which is consistent with the reaction taking longer to reach its maximum yield. When the copolymer with shorter blocks, $PMMA_7$-*b*-PEO_{17}, was used, the system behaved differently as illustrated in Figure 1(b). The single absorption peak noted above appears as a main peak at ~410 nm together with a broad 'shoulder' around 440 nm. Spectra with two broad peaks can be produced by AgNPs with diameters > 80-100 nm but such large particles seem unlikely in this case. The spectrum is suggestive of two distributions of particle sizes being produced with approximate sizes of 10-20 nm and of 50-60 nm. This could arise from the bimodal polymer distribution in (**6)** noted above although it seems unlikely given the similarity in chain length of the two components. While the λ_{max} values give only an approximate indication of NP size, they are consistent with the electron microscopy results discussed below.

Two major factors which control the size and arrangement of the nanoparticles in copolymer micelles are the micellar stability in the media and the strength of the interactions between the PEO block and the growing nanoparticles [22]. As with the gold nanoparticles produced in PS-*b*-PEO reported previously, the interactions here are relatively weak so that the micelles should not be affected significantly by the formation of the AgNPs and, in turn, the nanoparticle growth should not be greatly influenced. It may be that when short BCPs were used, this condition is not satisfied and that NP growth perturbed the smaller micelle structure to a greater extent.

The above observations were recorded during sonication. Previous work concerned with growing gold NPs in PS containing BCPs showed that the reaction continued to produce larger quantities of nanoparticles for some time after sonication stopped although significant amounts of agglomeration also occurred after longer times [21]. Figure 2(a) shows that the same

phenomena occur for AgNPs with the PS containing materials. The absorbance initially increases as more AgNPs form but then falls as the particles coalesce to form large clusters which settle out of solution and contribute no plasmon signal. In contrast, when PMMA was used as the hydrophobic block, no further change in the spectra occurred once sonication ceased (Figure 2b, 2c). The reasons for this difference in behaviour are not entirely clear but may be related to toluene being a thermodynamically better solvent for PS than for PMMA [29] with the consequence that little diffusion of reactants into the micelle core can occur through a 'tighter' PMMA layer without the impetus provided by the ultrasound. Silver nanoparticles also appear to be better stabilized by the copolymers than their gold equivalents and PMMA blocks are more effective at preventing further reaction, possibly due to stronger interactions of the methacrylate with the nanoparticles compared with the less polar styrene blocks.

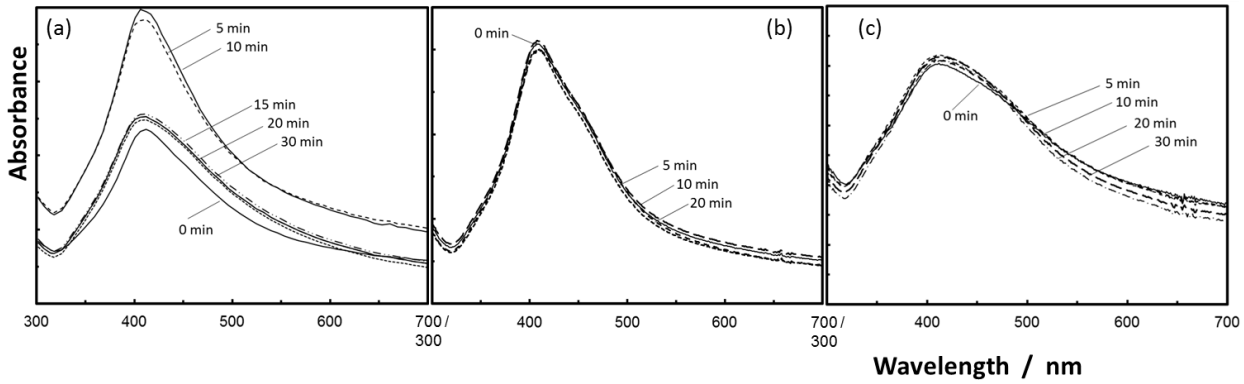

Fig. 2. Change in absorbance spectra after sonication was stopped. (a) Ag in PS_{61}-*b*-PEO_{113} (b) Ag in $PMMA_{50}$-*b*-PEO_{113} (c) Ag in$PMMA_{7}$-*b*-PEO_{17}

Given the different behaviour between the AgNPs formed with PS and PMMA blocks, it was prudent to reexamine the growth of gold NPs with the methacrylate containing copolymer to compare with previous work. The results are shown in Figure 3 with the characteristic plasmon absorption peak now shifted to around 540 nm. AuNPs form continuously through the 1 h

reaction time during sonication rather than passing through an optimum time as when PS blocks were involved. A broad absorption around 400-450 nm, the significance of which is not clear, appears at early reaction times but disappears as the reaction proceeds. As noted above, the growth appeared to be somewhat faster than with silver. When sonication is stopped, a small amount of further reaction takes place but, as with AgNPs, little aggregation in terms of a fall in absorbance was observed. This again suggests that PMMA is a more effective hydrophobic corona in stabilizing the nanoparticles even though the reaction takes place within the PEO micellar cores. It is thus clear that there are a range of subtle effects concerning the precise interactions of each block with the inorganic precursors and the solvent that control the growth of nanoparticles in these amphiphilic materials.

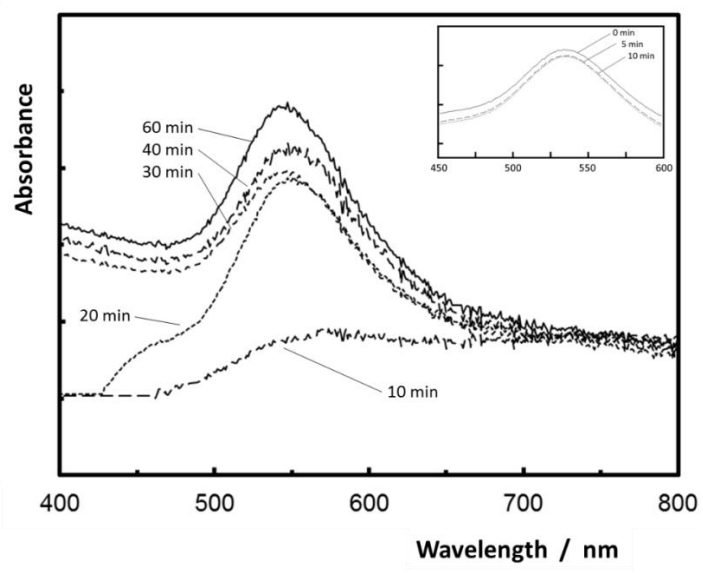

Fig. 3. Absorbance spectra at the indicated times during sonochemical reduction of $HAuCl_4$ in $PMMA_{50}$-*b*-PEO_{113}. Inset shows changes after sonication is stopped.

Further information on the resulting nanoparticles and the composite materials can be gained from electron microscopy. The morphology of the cast films of the NP containing block

copolymers was determined by SEM and is illustrated in Figures 4 and 5. The white spots represent silver particles. These results again indicate that the silver was well dispersed in the micelles. The micrographs are relatively featureless (except the large evaporation artefact in Figure 4) although it should be noted that no staining of the polymers was carried out. The dispersion of PS blocks in the PEO matrix is apparent (Figure 4), but the silver particles are much larger than the nanoparticles that initially form. Consideration of the UV spectra suggested that some agglomeration of the NPs occurred after formation and these electron micrographs add further evidence. At these length scales the distribution is less uniform than revealed by TEM. Reining and co-workers [30] have shown that the morphology of PEO-*b*-PS is highly dependent on the relative block lengths and on the details of sample preparation and the same comments appear to be true for the PMMA containing polymers shown in Figure 5. The major difference from Figure 4 is that the metal particles are not visible at these scales suggesting that a lower degree of agglomeration into large particles occurred when the hydrophobic block consisted of PMMA.

Representative TEM images of the AgNPs in the micellar block copolymers are illustrated in Figures 6 and 7. Here, the dark spots represent the micelle cores containing the silver nanoparticles. The micrographs indicate that the AgNPs were generally well dispersed in the micelles. The brighter areas between the dark spots represent the shells of the micelles which separate the silver nanoparticles so that not every micelle contained a nanoparticle. The images indicate that the nanoparticles are larger than the original cores and also than the remaining micelles suggesting that the PEO has been swollen by ingress of the silver nitrate. The size of the silver particles is in agreement with that suggested by the plasmon resonances, albeit at the lower end of the range.

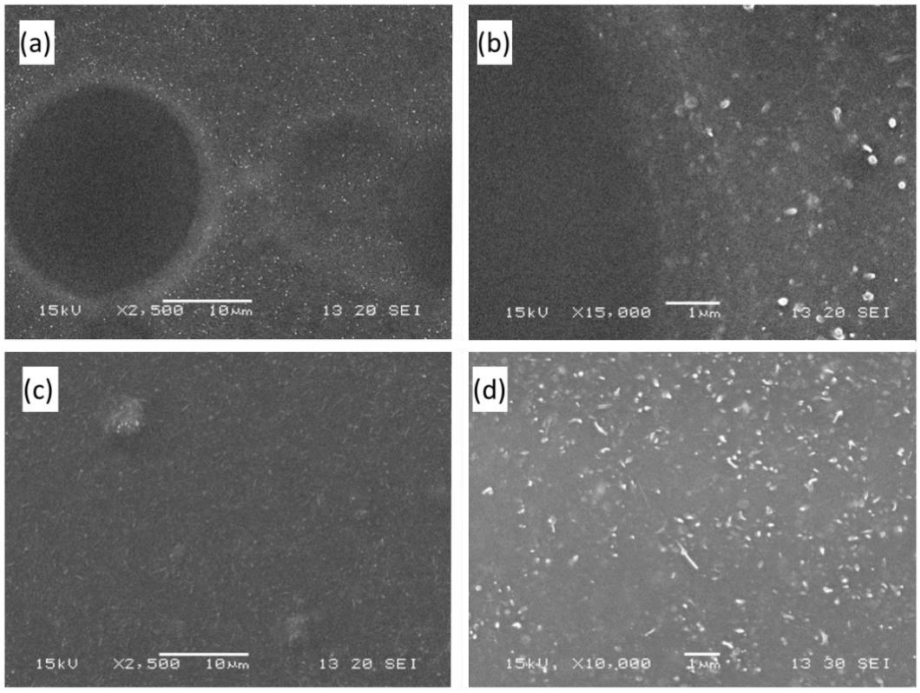

Fig. 4. SEM image for NPs in PS_{61}-*b*-PEO_{113}. (a), (b) AgNPs (c), (d) AuNPs.

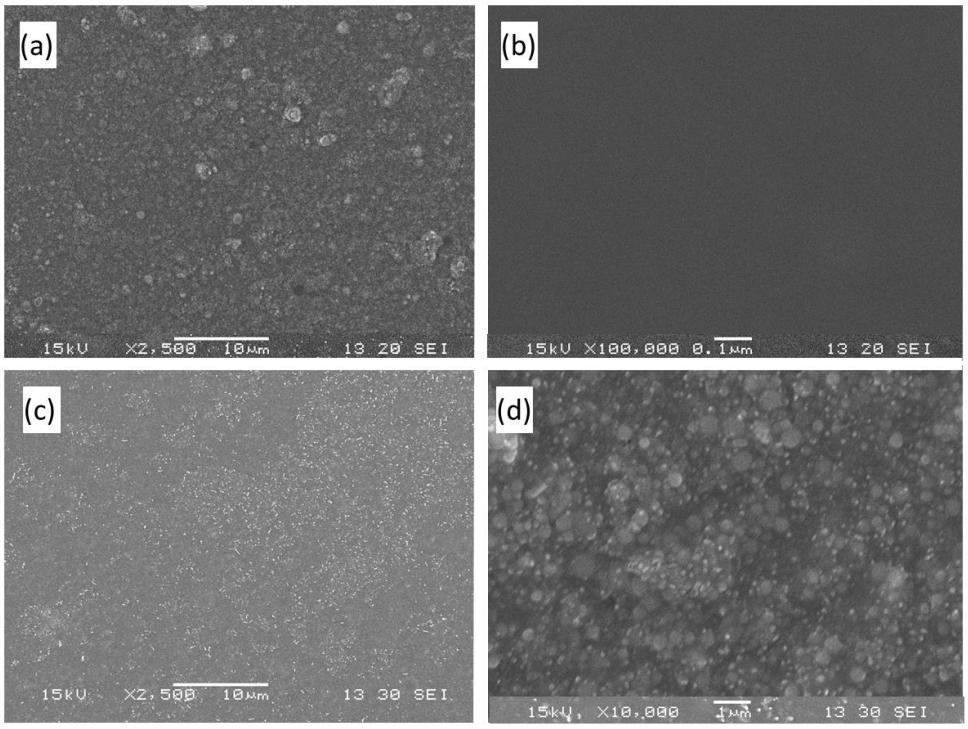

Fig. 5. SEM images for AgNPs. (a), (b) $PMMA_{50}$-*b*-PEO_{113} (c), (d) $PMMA_{7}$-*b*-PEO_{17}

For the results shown in Figure 6, the size of the PEO block is the same 113 repeat units in each case so that, as might be expected, the average AgNP size does not vary to a significant degree. While there is some evidence for a small degree of agglomeration of nanoparticles, this is much less than, for example, in the case of gold [26]. The distance between the AgNPs does change between the copolymers, possibly reflecting the changing PS block size. At high magnification, most particles appeared spherical (Figure 6(c)).

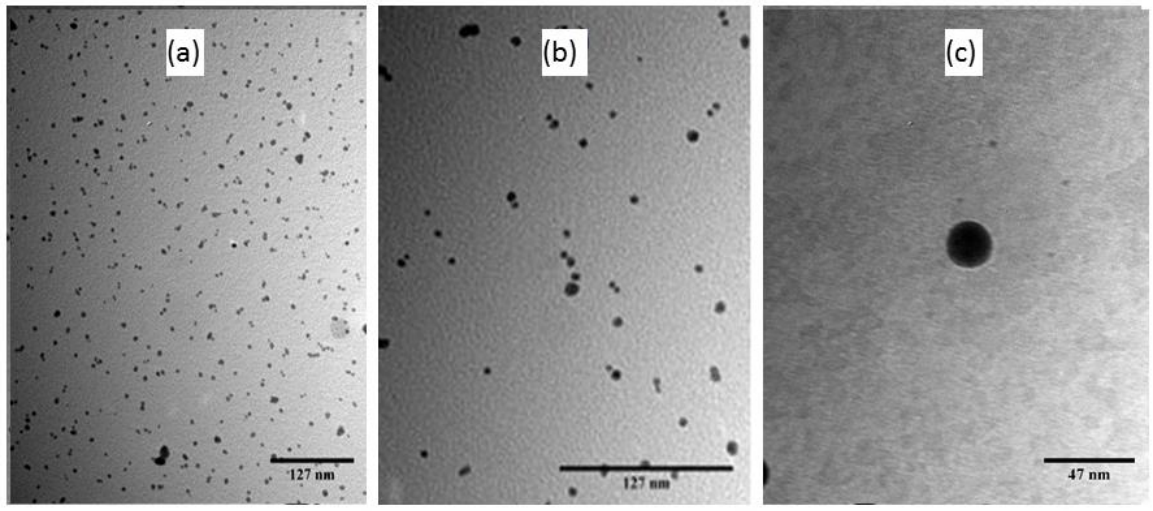

Fig. 6. TEM images for AgNPs in BCPs. (a) PS_{61}-*b*-PEO_{113} magnification 150000 (b) PS_{72}-*b*-PEO_{113} magnification 300000 (c) PS_{88}-*b*-PEO_{113} magnification 500000

Once again, more varied behaviour was observed with the range of PMMA-*b*-PEO copolymers shown in Figure 7, perhaps not unexpected given the variation in the PEO block size. There was greater variation in the AgNP size, larger blocks giving larger nanoparticles. There was also some evidence (Figure 7(b)) of adjacent micelles coalescing to yield 'dimeric' nanoparticles. For the copolymer with the smallest blocks, there is considerable variation in size and the TEM results (Figure 7(c)) add to the spectroscopic evidence above of a distribution containing both large and

small nanoparticles. The results further reinforce the above suggestion that PMMA stabilises the micelles and the solid copolymer film structure to a greater degree than polystyrene.

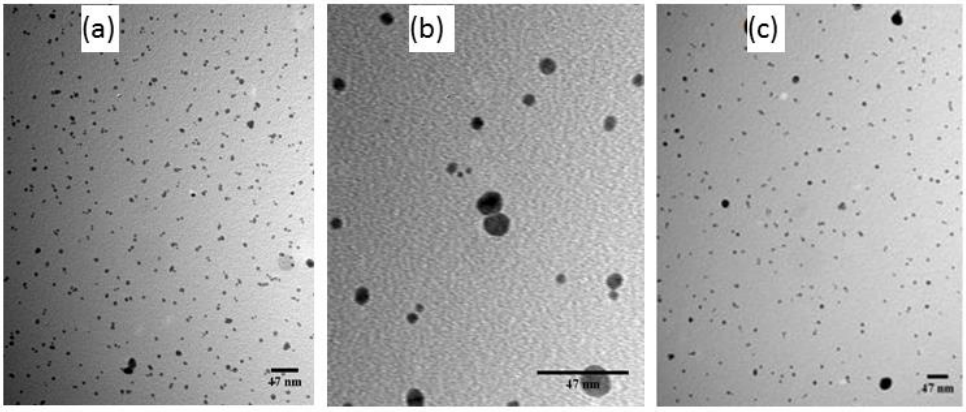

Fig.7. TEM image for AgNPs in BCPs (a) $PMMA_{50}$-*b*-PEO_{113} magnification 150000 (b) $PMMA_{50}$-*b*-PEO_{113} magnification 500000 (c) $PMMA_{7}$-*b*-PEO_{17} magnification 120000

Conclusions

This work confirms our previous findings with AuNPs in that the micellar structures formed by amphiphilic PS-*b*-PEO and PMMA-*b*-PEO block copolymers provide an excellent means for the formation of well-defined films containing nanoparticulate silver, the size of which can be controlled by variation of the sonication time and the hydrophilic block length as well as by the reaction time. Sonochemically enhanced borohydride reduction of silver nitrate is a rapid and controllable method for forming the silver nanoparticles and, in contrast to the production of gold by similar methods, the technique is more controllable. It produces more stable materials which are less prone to nanoparticle agglomeration. Other nanoparticles, for example platinum, palladium, TiO_2, Au or semiconductors, could be incorporated into micellar films using similar methodology; the use of mixed metal systems by using two (or more) precursors or by blending

the copolymers after NP preparation would also give an interesting avenue to extend the work. However, care must be taken to select the optimum reaction and processing time to achieve a balance between the individual nanoparticles and clusters. In particular, the sonication time must be optimised as prolonged reaction times lead to significant agglomeration with potential deterioration in optical performance.

Acknowledgments

One of the authors (I. Din) is highly thankful to the Higher Education Commission, Pakistan for their financial support. The authors are also grateful to the Center for Electron Optical Studies (Dr U. Potter) and the Department of Chemistry, University of Bath, for assistance with the electron microscopy and for providing laboratory facilities respectively.

References

1. Bhushan, B. (Ed.) (2010) Springer Handbook of Nanotechnology, ISBN 978-3-642-02524-2. Springer-Verlag, Heidelberg
2. Huang X, Xiao Y, Zhang W, Lang M (2012) Appl. Surf. Sci. 258(7):2655-60
3. Link S, El-Sayed MA (1999) J Phys. Chem. B 103(40):8410–8426
4. Kelly KL, Coronado E, Zhao LL, Schatz GC (2005) J. Nanosci. Nanotechnol 5(2):244-249
5. Chernousova S, Epple M (2013), Angew. Chem. Int. Ed 52:1636–1653
6. Reidy B, Haase A, Luch A, Dawson KA, Lynch I (2013) Materials 6(6):2295-2350
7. Bumbudsanpharoke N, Choi J, Ko S. (2015) J. Nanosci. Nanotechnol. 15(9):6357-72.
8. Sharma VK, Yngard RA, Lin, Y (2009) Adv. Coll. Interfac. Sci 145:83–96
9. Wojtysiak S, Kudelski A (2012) Colloids Surf. A: Physicochem. Eng. Asp 410:45–51
10. Wuithschick M, Paul B, Bienert R, Sarfraz A, Vainio U, Sztucki M, Kraehnert R, Strasser, Rademann PK, Emmerling F, Polte J (2013) Chem. Mater. 25(23):4679-89
11. Yakout SM, Mostafa AA (2015) Clin. Exptl. Med. 8(3):3538

12. Salkar RA, Jeevanandam, P, Aruna, ST, Koltypin, Y Gedanken, A (1999) J. Mater. Chem 9:1333-1335

13. Radziuk D, Shchukin D, Möhwald H (2008) J. Phys. Chem. C 112(7):2462–2468

14. Tang C, Lennon EM, Fredrickson GH, Kramer EJ, Hawker CJ (2008) Science 322(5900):429-32

15. Perelshtein I, Applerot G, Perkas N, Guibert G, Mikhailov S, Gedanken A (2008) Nanotechnol. 19(24):245705

16. Hamley IW (1998) The Physics of Block Copolymers¸ OUP, Oxford.

17. Haryono A, Binder WH (2006) Small 2(5):600–611

18. Sakai T, Alexandridis P (2004) Langmuir 20:8426–8430

19. Pizarro GC, Marambio OG, Jeria-Orell M, Olea A, Valdés DT, Geckeler KE (2013) J. Appl.Polym.Sci. 129(4):2076

20. Spatz JP, Roesher A, Möller M (1996) Adv. Mater. 8(4):337

21. Nawaz M, Ud-Din I, Price GJ, Baloch MK (2014) J. Polym. Res 21(8):1-7

22. Möller M, Spatz JP, Roescher A, Mossmer S, Selvan S, Klok HA (1997) Macromol. Symp. 117(1):207–218

23. I. Ud Din (2015) PhD Thesis, Hazara University, Mansehra, Pakistan; Manuscripts in preparation.

24. Matyjaszewski K (2012) Macromolecules 45:4015–4039

25. Nawaz M, Baloch MK, Price GJ, Ud-Din I, El-Mossalamy ES (2013) J. Polym. Res 20(7):1-8.

26. http://www.sigmaaldrich.com/materials-science/nanomaterials/silver-nanoparticles.html (accessed 16thSeptember 2016)

27. Sun Y, Xia Y (2002) Science 298(5601):2176-2179

28. Antonietti M (2003) Nature Mater. 2:9-10

29. Brandrup J, Immergut EH (Eds) (2003) The Polymer Handbook 4th Ed., J Wiley & Sons, New York

30. Reining B, Keul H, Höcker H (2002) Polymer 43(25):7145-54